Desalination and Water Treatment
www.deswater.com

doi: 10.1080/19443994.2016.1173377

57 (2016) 23085–23096
October

Taylor & Francis
Taylor & Francis Group

Quasi-steady state simulations of thermal vapor compression multi-effect distillation plants coupled to parabolic trough solar thermal power plants

Bartolomé Ortega-Delgado[a], Patricia Palenzuela[a], Diego C. Alarcón-Padilla[a,*], Lourdes García-Rodríguez[b]

[a]*CIEMAT-Plataforma Solar de Almería, Ctra. de Senés s/n, Tabernas (Almería) 04200, Spain, Tel. +34 950 387800; Fax: +34 950 365015; emails: bartolome.ortega@psa.es (B. Ortega-Delgado), patricia.palenzuela@psa.es (P. Palenzuela), diego.alarcon@psa.es (D.C. Alarcón-Padilla)*

[b]*Department of Energetic Engineering, Seville University, ETSI, Camino de los Descubrimientos s/n, Sevilla 41092, Spain, Tel. +34 954 487231; Fax: +34 954 487233; email: lourdesg@esi.us.es*

Received 4 May 2015; Accepted 25 February 2016

ABSTRACT

The evaluation of the coupling of a 50 MW_e parabolic trough solar thermal power plant (PT-STP) and a 10,000 m^3/d multi-effect distillation plant with thermal vapor compression (MED-TVC) was performed. To that end, a model for the entire system has been developed and implemented within Engineering Equation Solver (EES) and Matlab software environments. Two coupling arrangements between the PT-STP plant and the MED-TVC unit were selected: one taking low-pressure steam (at 1.224 bar) from the power block to feed the MED-TVC and the other one taking high-pressure steam (at 20.6 bar), and the simulations of the electricity and fresh water production of the PT-STP + MED-TVC plant to be located in Spain were carried out during three days in summer (21–23 June) and three days in winter (21–23 December). Results obtained showed that the use of the low-pressure steam to feed the MED-TVC plant reduces the electricity penalization compared with the use of high-pressure steam but also decreases the fresh water production. Since in Spain the electricity demand is lower in summer than in winter, and the contrary occurs with the fresh water demand, the optimum coupling arrangement in summer was using high-pressure steam to feed the MED-TVC (enough steam available in the turbines) and that one in winter was to feed the MED-TVC with low-pressure steam having the lower electricity penalization at the cost of the decrease of the fresh water production.

Keywords: Concentrating solar power; Desalination; Modeling; Multi-effect distillation; Parabolic trough

*Corresponding author.

Presented at EuroMed 2015: Desalination for Clean Water and Energy Palermo, Italy, 10–14 May 2015. Organized by the European Desalination Society.

1. Introduction

The increasing of the global population along with the rise in the agrarian and industrial activities are leading to a continuous growth of the electricity and water demands. This has become a significant issue in developing countries with emerging economies, like those within the BRICS (Brazil, Russia, India, China, and South Africa) group or those located in the Middle East, which will represent a major share of the worldwide population increase in the next decades.

Conventional power production systems based on fossil fuels are known to cause the global warming, mainly due to the CO_2 emissions to the atmosphere. Moreover, these systems rely on a limited source of energy (coal, oil, etc.) that will eventually run out. In this context, it is necessary the use of a mix of energy sources (conventional and renewable) to produce the power supply in the near future. Solar thermal power plants (STP) have been proved as reliable systems to produce electricity using solar irradiation as the energy source [1,2]. Its use has sense in regions of the world with high solar irradiation levels. Habitually, these zones also suffer from severe water stress (caused by the physical scarcity of fresh water or by the absence of facilities to extract the water from the natural sources) and they are located close to the sea. Therefore, the integration of STP and desalination plants, concept known as STP + D, represents an opportunity to partially solve the energy and water supply problems in these regions.

This paper analyses the integration of multi-effect distillation plants with thermal vapor compression (MED-TVC) into parabolic trough solar thermal power plants (PT-STP), based on the electricity and fresh water demands in Spain, which are variable during the year. The integration of the MED-TVC plant was made by taking steam from one of the extractions of the power block (PB) to feed the thermo-compressor. The comparison of the electricity production penalties and the fresh water production in different periods of the year, along with the suitability of using one coupling arrangement or another, is presented and discussed in this paper.

2. Methodology

The model of the whole system, PT-STP + MED-TVC plant, has been developed by modeling the three subsystems: the solar field, the PB, and the desalination unit. The details of each one are explained in the following sections. Two possible coupling arrangements between the PT-STP plant and the MED-TVC unit have been considered (as shown in Fig. 1): the first option consists in using steam from one of the extractions from the low-pressure turbine of the PB (E1–E4) to feed the MED-TVC while the second uses steam from one of the extractions from the high-pressure turbine (E5). Once the whole model has been developed, the simulation tool have been used to evaluate the thermal efficiency, the electricity, and the water production of the integrated plant during three representative days in summer and three representative days in winter.

2.1. Solar field

The solar field considered is a parabolic trough solar field for a STP plant of 50 MW_e (Andasol type) with oil (Therminol VP-1 [3]) as the heat transfer fluid (HTF) and thermal energy storage (TES, formed by two tanks with molten salts). It consists of 156 collector loops, with four solar collector assemblies (SCA) each one. One SCA is composed by 12 solar collector elements (SCE) with 28 glass facets each. The solar field has a north-south orientation for obtaining the maximum energy on a yearly basis. The collector is a Eurotrough 150 model with the characteristics described in Table 1.

The modeling of the solar field has been taken from [4], which has been validated with actual data from Andasol II, showing excellent agreement. It consists basically in applying an energy balance on a receiver control volume assuming a linear and discrete approximation over the governing differential equations in order to simplify the problem. Thus, the time step must be small enough, lower than 10 s, otherwise the error committed in the temperatures calculation would be significant. This model considers the solar field as a closed circuit with all the collectors equally disposed and an insulated pipe for the HTF distribution. Each day is divided into four periods: a night time period before the sunrise, a start-up period for warming the HTF and initiate the PB operation, a full operation period up to the sunset, and a second night time period. The HTF temperatures in each collector and in the insulated pipes are supposed to be uniform and they are obtained by iteration starting from the initial guesses.

The model uses data of the direct normal irradiance, ambient temperature, and wind velocity from a typical meteorological year generated by the software Meteonorm [5], being the average yearly solar irradiation and ambient temperature in good agreement with actual data provided by a solar station located in the

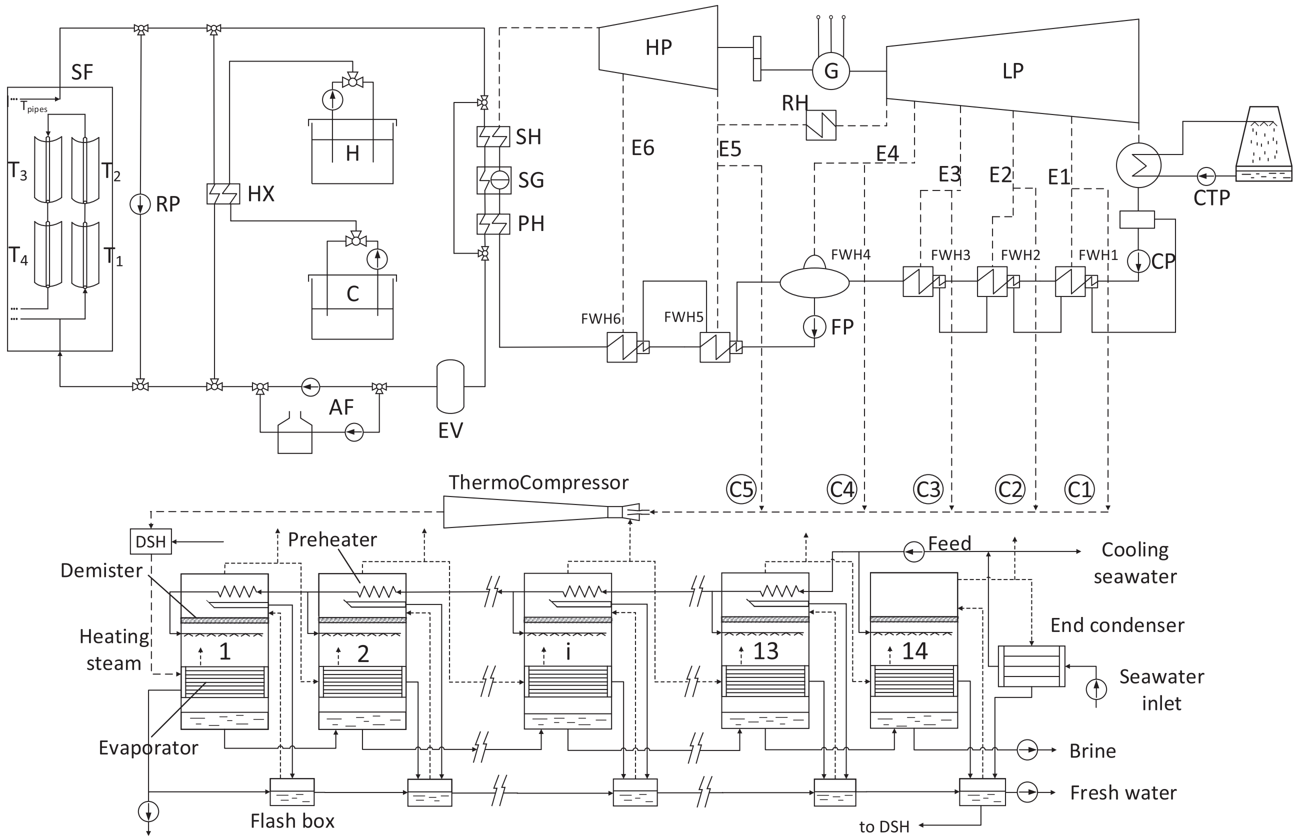

Fig. 1. Scheme of the overall system where the different alternatives to feed the thermo-compressor (C1 to C5) are represented.

Notes: AF = anti-freeze system; C = cold tank; CP = condensate pump; CTP = cooling tower pump; DSH = desuperheater; E1-E6 = turbine steam extractions; EV = expansion vessel; FP = feeding pump; FWH = feedwater heater; G = electric generator; HX = heat exchanger; HP = high-pressure turbine; H = hot tank; LP = low-pressure turbine; PH = preheater; RP = recirculating pump; RH = reheater; SF = solar field; SG = steam generator; SH = superheater; T = temperature.

selected area. The plant was considered to be located in Almería, SE of Spain (longitude 2.215W and latitude 37.06N). The design inlet and outlet HFT temperatures in the solar field were 296–390˚C, respectively. It was considered a maximum limit for the thermal energy absorbed by a collector loop (1.8 MW_{th}), which guarantees not to surpass the maximum design value of the outlet HTF temperature, and for the thermal power sent to the PB (140 MW_{th}), which corresponds to a maximum net electric power of 50 MW_e. Notice that during the only-TES operation there is a decrease in the electricity production since the maximum limit for the energy sent to the PB was established at 119 MW_{th} because the temperature of the salts is lower than the HTF temperature. Following the same operation strategy as in [4], it was assumed that the steam generator starts to produce steam for the electricity generation once the HTF outlet temperature is 310˚C.

2.2. *Multi-effect distillation plant with thermal vapor compression*

The design of this system is based on the MED-TVC plant located in Trapani (Italy) [6]. The plant consists basically of 14 effects, 13 preheaters, and 14 flashing boxes, in parallel-cross feeding arrangement (Fig. 2). The process is based on the evaporation of the seawater and subsequent condensation of the vapors formed, considered free of salts. This process takes place inside pressurized vessels, called effects, which are composed by three main elements: an evaporator, a demister, and a preheater. The thermal input required by the process is added exclusively in the first effect, called heating steam, which flows inside the tube bundle of the evaporator. The seawater is sprayed over the outer surface of the evaporator tubes, evaporating part of it due to the heat released by the condensation of the heating steam. The vapors formed go through the demister, where the droplets are

Table 1
Characteristics of the ET-150 solar collector [4]

Concept	Value
Gross length (m)	150
Net length (m)	142.8
Gross aperture width (m)	5.77
Net aperture area (m^2)	817.5
Focal length (m)	1.71
Absorber radius (m)	0.035
Mirror reflectivity ρ	0.932
Receiver glass transmissivity τ	0.96
Absorbance of the metallic pipe (selective coating) α	0.95
Reduction of the effective absorbing receiver length	0.954
Reduction in the energy absorbed by the receiver due to inaccuracies in the assembly	1
Peak optical efficiency $\eta_{opt,0}$	0.81
Spacing between rows (m)	17.2
Spacing between consecutive SCAs in a row (m)	1.5
Spacing between consecutive SCEs in a SCA (m)	0.25
Number of SCAs in a row	2
Number of SCEs in a SCA	12

retained, and part of it condenses in the preheater, warming up the feed seawater. The rest of the vapor is driven inside the tubes of the next evaporator, repeating the process. The vapor condensed (from the evaporator and preheater) is collected inside the flashing boxes, where additional flash vapor is produced. The last effect does not have preheater associated but a final condenser. The thermal efficiency of the system can be improved by recompressing part of the vapors formed, using a thermo-compressor. This device is very simple and robust. It uses high-pressure steam (called motive steam) to compress low-pressure vapor (called suction steam) taken from one of the MED plant effects by the Venturi effect. The vapor at the outlet (called compressed vapor) is a mixture of both vapors and it is at an intermediate pressure.

The mathematical model was developed at steady state and was implemented in the EES [7] environment. It is based on the mass and energy balances applied to the different elements of the plant, along with the heat transfer equations corresponding to the heat exchangers. The input data for the model are detailed in Table 2. As output data, the areas of the heat exchangers, the distillate production, and the efficiency of the plant were obtained. The latter parameter is defined by the Gain Output Ratio (GOR) which is determined as the ratio of total distillate mass flow rate produced (q_D) to the mass flow rate of motive steam entering the thermo-compressor (q_m):

$$\mathrm{GOR} = \frac{q_D}{q_m} \quad (1)$$

For the model of the thermo-compressor, the correlations obtained by Hassan et al. [8], which are suitable for a wide range of operation conditions of the motive steam pressure, were used.

Moreover, a parametric study as function of the motive steam and suction steam pressures was carried out in order to obtain the best coupling arrangement with a PT-STP plant, in terms of the GOR of the MED-TVC plant and the efficiency in the electricity production of the PT-STP plant. The motive steam pressures studied were selected from the STP plant referenced in [9]. Such study was made for optimum values of the specific heat transfer areas (that ones that minimize the heat transfer areas of the effects located after of the thermo-compressor location). It was selected two scenarios in order to match with the variability in the electricity demand: steam extracted from

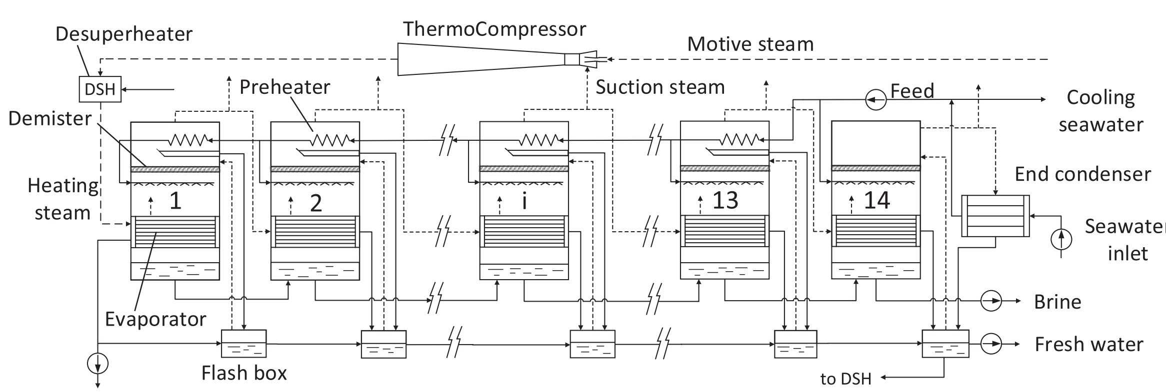

Fig. 2. Scheme of the MED-TVC plant.

Table 2
Main inputs for the design of the MED-TVC plant

Parameter	Value
Design capacity[a] (m^3/d)	10,000
Number of effects	14
Heating steam temperature (°C)	70
Intake seawater temperature (°C)	25
Intake seawater salinity (ppm)	35,000
Rejected brine temperature (°C)	37
Maximum brine salinity (ppm)	60,000
Temperature difference in final condenser (°C)	10
Desuperheater outlet temperature (°C)	73
Diameter of the tubes between the effects (mm)	600
Tube longitude between the effects (m)	2
Tube longitude in evaporators (m)	7
External diameter of evaporator tubes (m)	0.038
Internal diameter of evaporator tubes (m)	0.031
Wire diameter of demisters (mm)	0.28
Density of demisters (kg/m^3)	280
Mesh pad thickness (m)	0.15

[a]Taking as suction steam that one from the last effect of the MED plant.

E2 (1.224 bar) and from E5 (20.6 bar) bleeds as motive steam to feed the MED-TVC plant (Fig. 1).

For the simulation of the integrated PT-STP + MED-TVC plant at partial load operation, it has been supposed that the change in the motive steam mass flow rate is directly proportional to the steam cycle mass flow rate and that the GOR is maintained constant and equal to that one obtained from the parametric analysis in each scenario.

2.3. Power block

The PB corresponds to a regenerative Rankine cycle with reheating and six extractions, for a net power production of 50 MW_e (Fig. 3). It consists of two turbines,

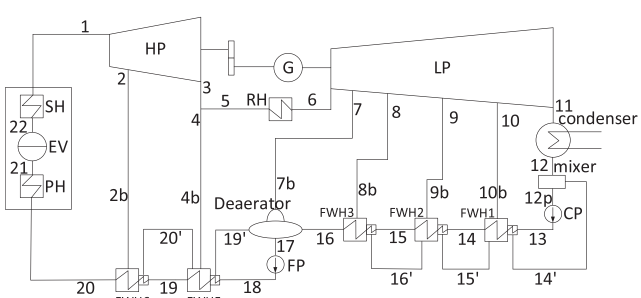

Fig. 3. Scheme of the PB.
Notes: CP = condensate pump; FP = feeding pump; FWH = feedwater heater; G = electric generator; HP = high-pressure turbine; LP = low-pressure turbine; PH = preheater; RH = reheater; SH = superheater.

high pressure and low pressure turbines, coupled to an electrical generator (at different rotational speeds), a steam generator composed of a preheater, an evaporator, a superheater and a reheater, five closed feedwater heaters, one open feedwater heater (deaerator), a water-cooled condenser (with evaporative tower), two centrifugal pumps: the condensate pump and the feeding pump, and a condensate mixer. The model, which was implemented in EES environment, takes into account the part load operation of the cycle using the equations reported by Montes et al. [9].

Firstly, the cycle was solved under nominal conditions using the inputs of the Table 3. For this purpose, each point of the cycle was defined by calculating its thermodynamic properties, temperature, pressure, specific enthalpy, and specific entropy, along with the steam mass flow rate. The thermal efficiency of the cycle at nominal conditions was also determined as follows:

$$\eta_{\mathrm{th}} = \frac{W_{\mathrm{u}}}{(h_1 - h_{20}) + (h_6 - h_5) \cdot (1 - \alpha_2 - \alpha_4)} \quad (2)$$

where W_{u} is the useful mechanical energy generated in the cycle (equal to the energy obtained in the HP and LP turbines minus the energy consumption of the pumps), in kJ/kg, h is the specific enthalpy of the steam, in kJ/kg and α is the fraction of the total mass flow rate used in each extraction.

At part load conditions, the efficiencies of all the elements of the cycle are reduced. Particularly, the turbine efficiency was determined according to Bartlett's equation [10]:

$$\%\ \text{Reduction} = 0.191 - 0.409\left(\frac{q_{\mathrm{v}}}{q_{\mathrm{v,ref}}}\right) + 0.218\left(\frac{q_{\mathrm{v}}}{q_{\mathrm{v,ref}}}\right)^2 \quad (3)$$

$$\eta_{\mathrm{s},t} = (1 - \%\ \text{Reduction}) \cdot \eta_{\mathrm{s},t,\mathrm{ref}} \quad (4)$$

where q_{v} and $q_{\mathrm{v,ref}}$ are the total steam mass flow rates flowing in the cycle in actual and nominal operation, in kg/s, respectively. In Eq. (4) $\eta_{\mathrm{s},t}$ and $\eta_{\mathrm{s},t,\mathrm{ref}}$ are the isentropic efficiencies of the turbine in actual and nominal operation, respectively.

There are several control strategies for a steam turbine working in off-design conditions. The sliding pressure method has been established, which maintains fixed steam temperature at the inlet of the turbine and varies the mass flow rate with the steam pressure in the steam generator, using wide open control valves at the governing stage. Therefore, when the PB is working at part load conditions, the steam

Table 3
Characteristics of the power block at nominal conditions [9]

Parameter	Value
Turbine	
Inlet temperature (°C)	370
Inlet pressure (bar)	90
High-pressure turbine efficiency (%)	85.5
Low-pressure turbine efficiency (%)	89.5
Electro-mechanical efficiency (%)	98
Condenser	
Pressure (bar)	0.08
Extraction point pressures	
Point 2 (bar)	45.4
Point 4 (bar)	20.6
Point 7 (bar)	8.75
Point 8 (bar)	3.627
Point 9 (bar)	1.224
Point 10 (bar)	0.346
Pressure drop	
Extraction line no. 1 (%)	2.5
Extraction line no. 2 (%)	3
Extraction line no. 3 (%)	4.5
Extraction line no. 4 (%)	3
Extraction line no. 5 (%)	3
Extraction line no. 6 (%)	3.5
Reheating line (%)	11.75
Condenser pump	
Isentropic efficiency (%)	75
Electro-mechanical efficiency (%)	98
Feedwater pump	
Isentropic efficiency (%)	78
Electro-mechanical efficiency (%)	98
Closed feedwater heaters	
Terminal temperature difference (°C)	1.5
Drain cooling approach (°C)	5
Steam generator	
Thermal efficiency (%)	98
Total pressure drop (water side) (bar)	4.5

pressure and the mass flow rate of steam decrease, along with the extraction pressures. This pressure drop can be obtained using the Law of the Ellipse of Stodola [11], rearranged as function of the steam pressures and mass flow rates between any two points of the turbines 1 and 2:

$$\frac{p_1^2 - p_2^2}{p_{1,\mathrm{ref}}^2 - p_{2,\mathrm{ref}}^2} = \left(\frac{q_\mathrm{v}}{q_{\mathrm{v,ref}}}\right)^2 \tag{5}$$

The generator efficiency also changes at part load operation, and it was obtained using the equation reported by [12] for the SEGS VI power plant:

$$\eta_\mathrm{gen} = 0.908 + 0.258 \cdot \mathrm{Load} - 0.3 \cdot \mathrm{Load}^2 + 0.12 \cdot \mathrm{Load}^3 \tag{6}$$

where Load is the fraction from nominal operation (expressed in parts per unit).

The closed feedwater heaters have lower efficiency when the load decreases. Patnode [12] derived the following expression to calculate the UA factor working at part load operation, assuming constant fluid properties, neglecting the fouling and thermal resistance through the tubes, fully developed and turbulent flow inside the tubes and same proportion of the mass flow rates of inner and outer fluids at nominal and part load operation:

$$\frac{\mathrm{UA}}{\mathrm{UA_{ref}}} = \left(\frac{q_\mathrm{v}}{q_{\mathrm{v,ref}}}\right)^{0.8} \tag{7}$$

Finally, the efficiency of the pumps at the part-load operation was determined as function of the mass flow rate (equation reported by Lippke [13]):

$$\frac{\eta_\mathrm{s}}{\eta_{\mathrm{s,ref}}} = e_{\mathrm{m,ref}} + 2\left(1 - e_{\mathrm{m,ref}}\right)\frac{q_\mathrm{v}}{q_{\mathrm{v,ref}}} - \left(1 - e_{\mathrm{m,ref}}\right)\left(\frac{q_\mathrm{v}}{q_{\mathrm{v,ref}}}\right)^2 \tag{8}$$

where $\eta_{\mathrm{s,ref}}$ is the isentropic efficiency of the pumps at nominal conditions and $e_{\mathrm{m,ref}}$ a parameter related to the efficiency curves of the pumps [13] (for constant speed pumps $e_{\mathrm{m,ref}} = 0$).

Notice that there is a technical minimum of the thermal input from the solar field below which the turbine is stopped and the electricity production is zero. In this work, this value was chosen to be roughly 41 $\mathrm{MW_{th}}$ (30% of the nominal load). The results of the PB performance at nominal and part load operation, in only-electricity mode, can be seen in Appendix 1.

3. Results

As preliminary results from the parametric analysis mentioned in Section 2.2 needed to perform the simulations of the integrated PT-STP + MED-TVC plant, it was found that for a motive steam pressure of 20.6 bar, corresponding to the steam extraction at the outlet of the high pressure turbine (C5), the

Table 4
Parametric analysis of the GOR as function of the motive steam pressure and thermo-compressor location

p_m	N							
bar	6	7	8	9	10	11	12	13
20.6	16.37	16.45	16.57	16.71	16.86	17	17.08	17.04
1.224	13.71	13.79	13.81	13.68	13.65	13.58	13.44	13.23

maximum GOR of the TVC-MED unit (17.08) resulted for the case that the thermo-compressor takes the suction steam from the 12th effect of the MED plant. For a motive steam pressure of 1.224 bar, taken from an intermediate extraction of the low-pressure turbine (C2), the maximum GOR (13.81) was obtained for the case that the suction steam is taken from the 8th effect of the MED plant (Table 4).

The results of the simulations of the integrated PT-STP + MED-TVC plant are shown in Figs. 4–10. Note that the results and discussion presented here are totally dependent on the location selected. They can be representative for locations with ambient conditions similar to that one selected (Mediterranean area), but they would be different for other locations with other climatic conditions. Fig. 4 shows the thermal efficiency of the Rankine cycle in only-electricity and electricity plus water modes, being the MED-TVC plant fed by the C2 or C5 steam extractions from the LP and HP turbines, respectively. As it can be seen, in both cases the electricity generation is penalized when the MED-TVC unit is integrated in the PB of the STP plant due to the use of steam extracted from the turbine, which is not further expanded in the following turbine stages, to feed the MED-TVC unit. In the case of using the C2 extraction for the MED-TVC plant, the efficiency of the Rankine cycle under nominal conditions is approximately decreased two percentage points in comparison with the efficiency in the only-electricity mode. In the case in which the C5 extraction is taken for the MED-TVC plant, the reduction is doubled with respect to the previous case resulting in a decrease of four percentage points compared to the only-electricity mode.

This analysis suggests that if the electricity demand is high, the MED-TVC unit should be fed by the C2 extraction as it produces the lower decrease in the thermal efficiency of the cycle and the penalization in the electricity production is minimal. On the contrary, if the electricity demand is low and there is high-pressure steam available to feed the MED-TVC plant, the optimum integration would be using the C5 extraction as the GOR is significantly improved.

The simulation of the solar field for the three days in summer (21–23 June) is depicted in Fig. 5 by considering the starting point with no energy stored. In this figure, the HTF temperatures in the four collectors of each loop are represented ($T_1 - T_4$), along with the HTF temperature in the insulated pipes (T_{pipes}), the direct normal irradiance (E_b), the excess of thermal power generated by the solar field ($P_{PBexcess}$, which is sent to the thermal storage system), the energy stored in the TES (E_{stored}), the useful thermal power produced by the solar field ($P_{SFuseful}$), the useful thermal power sent to the PB ($P_{PBuseful}$), and the mass flow rate of HTF flowing in each loop (q_{loop}).

It can be observed that the irradiance profile of the first day was irregular, which was caused by the presence of clouds. However, the useful thermal power sent to the PB reached nominal values (140 MW_{th}). The sunrise took place at 5:47 UT and the useful thermal power sent to the PB started to be generated at 7:28 UT. Nevertheless, the electricity was generated only when this thermal power was above the technical minimum for the turbines, 41 MW_{th}, at 8:45 UT (see Fig. 6). As can be seen, during this day, the TES was charged up to around 200 MWh, which means a 20% of its full capacity, 1,010 MWh. The TES is charged only when there is excess of thermal power in the collectors (cyan line in Fig. 5) and discharged only when the useful thermal power collected in the solar field

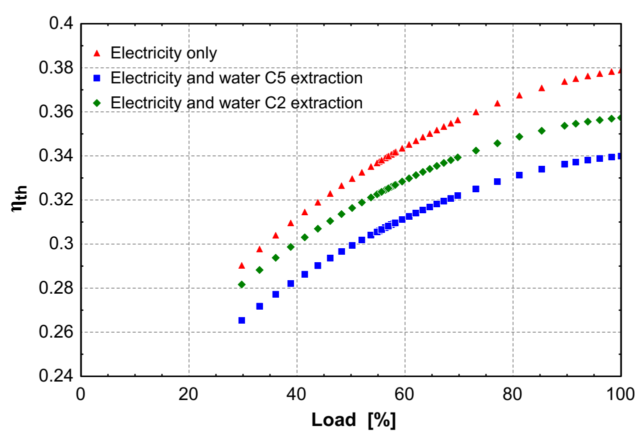

Fig. 4. Comparison of the thermal efficiency of the PB as function of the load for electricity-only and electricity plus water operation modes (with the MED-TVC fed by the C2 and C5 extractions).

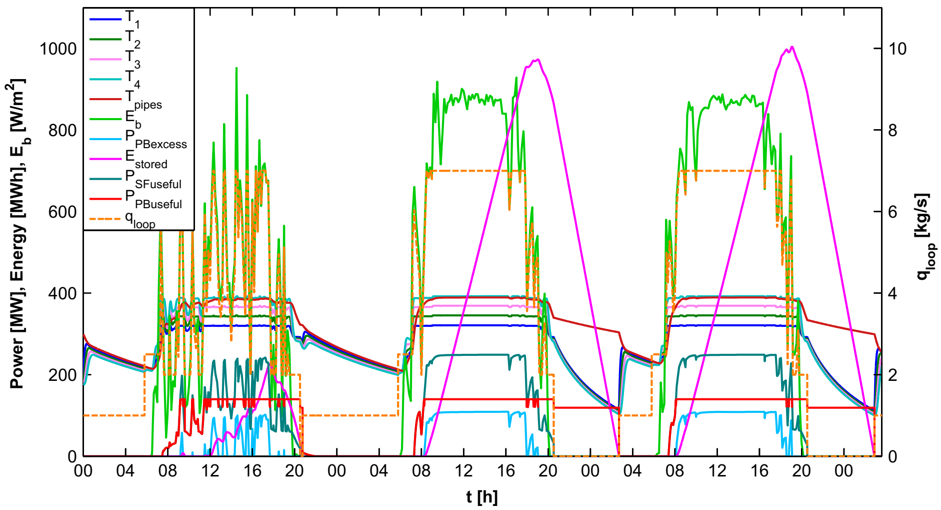

Fig. 5. Simulation of the solar field for three days in summer: 21–23 June.

(green line) is below the nominal value, if possible. From 17:39 to 20:45 UT approximately the TES started to be discharged and the operation was mixed with the operation of the solar field. The other two days simulated showed a better irradiance profile resulting in a nearly constant operation and more electricity production as a result of the useful thermal energy sent to the PB (red line), which is increased by the only-TES operation mode after the sunset (extending the electricity production up to 7.5 h until 3 AM approximately).

Figs. 6 and 7 show the electrical energy and fresh water production during the mentioned summer days (W_{eT} and q_{DT}) along with the daily fresh water production (q_{Dm3d}) and the electrical power ($\dot{W}_e$) with the MED-TVC fed by the low (C2) and high (C5) pressure extractions, respectively. As can be observed, the maximum values of electricity production are reached during the daylight hours (from 8 AM UT up to 20 PM UT approximately) due to the high irradiance values that are obtained in these periods (see Fig. 6). The maximum electricity production using C2 extraction was 47.63 MW_e (a 5% less than in the electricity-only operation mode) while it was 45.05 MW_e when C5 extraction was considered (a 10% less in comparison with the electricity-only operation mode). For the fresh water, the maximum production was 8,872.6 m^3/d using the C2 extraction and 9,938.6 m^3/d when the C5 extraction was used (11.27 and 0.6% less than the nominal value, respectively). On June 21, the operation of the integrated plant did not continue after the sunset due to the TES was discharged before that moment. However,

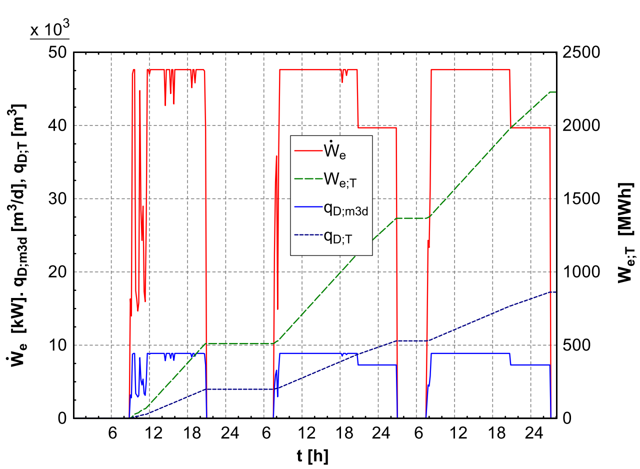

Fig. 6. Electricity and water production for three days in summer (21–23 June) (with the MED-TVC fed by the C2 extraction).

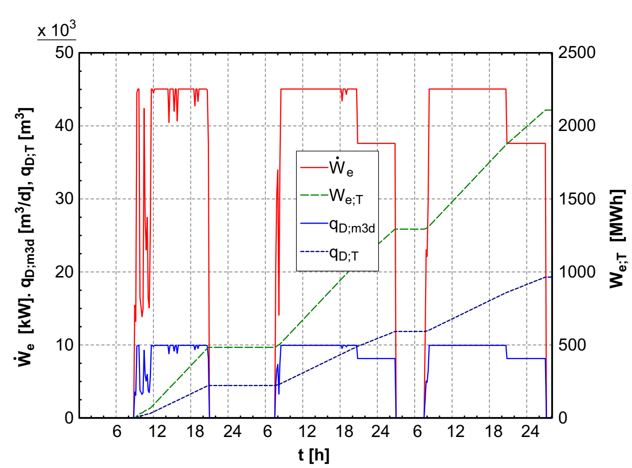

Fig. 7. Electricity and water production for three days in summer (21–23 June) (with the MED-TVC fed by the C5 extraction).

on 22–23 of June, the integrated PT-STP + MED-TVC plant continued operating after the sunset thanks to the TES (Fig. 6), although the electricity production was lower due to the lower thermal input to the PB from the TES. As it can be seen, the water production followed the same trend as the electricity production.

The total electricity and fresh water production during the three days was 2,228 MWh and 17,243 m^3 when the C2 extraction was considered and 2,108 MWh and 19,293 m^3 when using the C5 extraction, respectively. Therefore, the electricity production was penalized a 5.38% when the high-pressure steam from the turbine is used to feed the MED-TVC plant with respect to the case of taking low-pressure steam. However, the water production was improved by 11.89% regarding the low-pressure extraction and, as mentioned above, in this case the efficiency of the plant was higher (with a GOR of 17.08). As in Spain the electricity demand is lower in summer than in winter and the fresh water demand has the opposite trend, it seems suitable to use the C5 extraction in summer when the desalination plant produces higher amount of water at a higher efficiency, at the expense of reducing the electricity production.

Similar analysis was carried out for the three days in winter (21–23 December). Fig. 8 shows the output parameters of the solar field for the three days. As depicted, the irradiance profiles were very irregular, and the useful thermal power generated by the solar field in this period was quite low. The TES system was not charged in any of the days, being the daily operation reduced to the period up to few hours as long as there was useful thermal power to be sent to the PB and it was above the technical minimum considered for the turbines operation (41 MW$_{th}$). The sunrise took place at 8:17 UT in this period but there were not useful thermal power until 12:56 UT in the first day. However, the electricity production started only when the useful thermal power sent to the PB reached 41 MW$_{th}$ at 16:27 (Fig. 9). The turbines were stopped at 17:09 UT in this first day because the useful thermal power fell below 41 MW$_{th}$ at that time. In this day, the plant generated electricity only during roughly half an hour. The plant's operation during the other two days followed similar behavior.

Figs. 9 and 10 show the electricity and fresh water production during this period for both the C2 and C5 coupling arrangements. When the MED-TVC plant is coupled to the PT-STP plant by the C2 extraction, the total electricity production was 202.6 MWh and the maximum electrical power generated was 40.72 MW$_e$, while in the case of using the C5 extraction, the electricity production decreased to 191.8 MWh and the maximum value reached was 38.57 MW$_e$. Regarding the total fresh water production, it was 1,605–1,782 m^3 for the C2 and C5 arrangements, and the maximum values obtained were 7,480.3–8,352.9 m^3/d, respectively.

From the results obtained in this period, it follows that using the high-pressure extraction to feed the MED-TVC plant, the electricity production was penalized by 5.33% with respect to the use of the low-pressure extraction. The fresh water generated was increased by 11%. As the electricity demand in Spain is higher in winter and during this period there is less high-pressure steam available to feed the MED-TVC (because the PB works almost all the day at part load

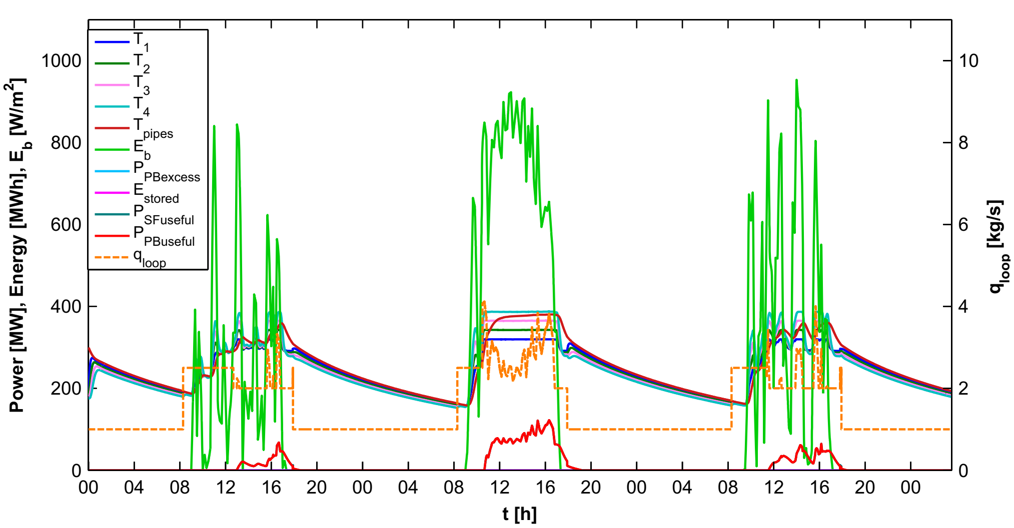

Fig. 8. Simulation of the solar field for three days in winter: 21–23 December.

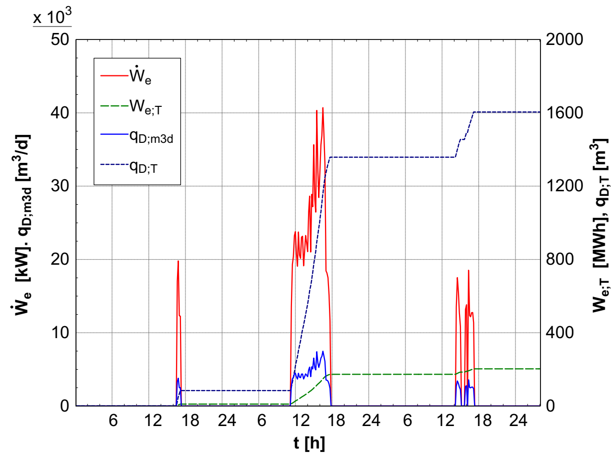

Fig. 9. Electricity and water production for three days in winter (21–23 December) (with the MED-TVC fed by the C2 extraction).

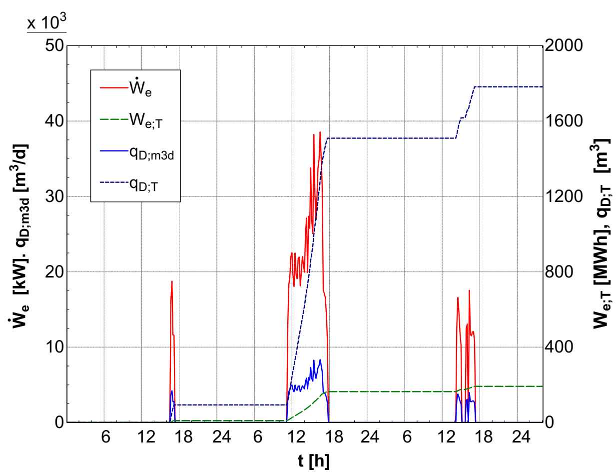

Fig. 10. Electricity and water production for three days in winter (21–23 December) (with the MED-TVC fed by the C5 extraction).

operation and consequently the pressures and mass flow rates of steam are lower) it would be more convenient to use low-pressure steam from the C2 extraction of the turbine as the heat source of the MED-TVC unit.

4. Conclusions

It has been developed a simulation tool for the fresh water production with MED-TVC systems that is useful to select, depending on the electricity and fresh water demand profile, which is the optimal coupling arrangement from the energetic point of view (maximum GOR of the MED-TVC unit and thermal efficiency in the electricity generation).

The model has been used to simulate the electricity and fresh water production of a PT-STP-MED-TVC plant during three representative days of summer (21–23 June) and winter (21–23 December). Firstly, parametric study of the GOR of the MED-TVC unit as function of the motive steam pressure and thermo-compressor location was carried out, using data from Andasol II power plant. Two scenarios were selected as result of the parametric analysis: the first coupling arrangement considered was to feed the MED-TVC with a high-pressure steam extraction of 20.6 bars and with the thermo-compressor located in the 12th position, which produced a maximum GOR of 17.08, but at the same time considerably penalized the electricity production. The second coupling arrangement consisted in using a low-pressure steam extraction of 1.226 bar and with the thermo-compressor located in the 8th position (which maximized the GOR to 13.81), and produced a lower impact on the electricity generation.

The results of the simulations showed that when the MED-TVC unit was fed by the high-pressure steam extraction from the turbine, the fresh water production was improved by 11.89% for the three days of summer and by 11% during the three days of winter compared to the case of using the low-pressure steam extraction. In the case of the electricity production, it was penalized a 5.38 and a 5.33% in summer and in winter, respectively, when using steam at 20.6 bar compared with the use of steam at 1.226 bar. Although the results were similar for the two periods analyzed, the selection of one or another coupling arrangement for the PT-STP-MED-TVC plant depends on the electricity and water demands in the location considered. During the three days of summer it was produced 2,228 and 2,108 MWh of electrical energy using the C2 and C5 steam extractions, respectively, while in the three days of winter the production was 202.6 and 191.8 MWh, which mean a 90.9 and a 91% lower than in summer. Particularly, in Spain, the highest electricity consumption takes place in winter, when the weather conditions are worse and the fresh water demand is low. During this period, it is then recommended the use of a low-pressure extraction of the LP turbine, which produces the lower penalization in the electricity generation although the fresh water production is reduced. On the contrary, in summer in Spain the electricity demand is lower and the water demand is higher. It is recommended thus for this period to integrate the MED-TVC unit into the PT-STP plant using a high-pressure steam extraction from the HP turbine, which produces more fresh water at the expense of penalizing the electricity production.

Acknowledgments

The authors wish to thank the European Commission (DG for Research and Innovation) for its financial assistance within the Integrated Research Programme in the field of Concentrated Solar Power (CSP) (STAGE-STE Project; Grant Agreement no. 609837).

Nomenclature

Abbreviations

AF	—	anti-freeze system
BRICS	—	Brazil, Russia, India, China, and South Africa
C	—	cold tank
CP	—	condensate pump
CSP	—	concentrating solar power
CSP + D	—	concentrating solar power and desalination
CTP	—	cooling tower pump
DSH	—	desuperheater
EES	—	engineering equation solver
EV	—	expansion vessel
FWH	—	feedwater heater
G	—	electric generator
GOR	—	gain output ratio
H	—	hot tank
HCE	—	heat collection elements
HP	—	high-pressure turbine
HTF	—	heat transfer fluid
HX	—	heat exchanger
LP	—	low-pressure turbine
MED	—	multi-effect distillation
PB	—	power block
PC	—	parallel-cross
PH	—	preheater
PT	—	parabolic trough
RH	—	reheater
SCA	—	solar collector assembly
SCE	—	solar collector element
SF	—	solar field
SG	—	steam generator
SH	—	superheater
STP	—	solar thermal power
TES	—	thermal energy storage
TMY	—	typical meteorological year
TVC	—	thermal vapor compression

Symbols

p	—	pressure (bar)
E	—	irradiance (W/m^2)
h	—	specific enthalpy (kJ/kg)
q	—	mass flow rate (kg/s)
T	—	temperature (°C)
UA	—	heat exchanger constant (kW/m^2 °C)
W	—	specific energy (kJ/kg)

Greek symbols

α	—	fraction of the total mass flow rate used in each extraction
β	—	reduction of evaporator areas after the thermo-compressor extraction
η	—	efficiency
τ	—	receiver glass transmissivity

Subscripts

b	—	direct normal
D	—	distillate
gen	—	generator
m	—	motive
opt	—	optical
ref	—	reference
s	—	isentropic
T	—	total
t	—	turbine
th	—	thermal
u	—	useful
v	—	vapor

References

[1] NREL, TroughNet–US Parabolic Trough Power Plant Data, 2015. Available from: <http://www.nrel.gov/csp/troughnet/power_plant_data.html> (accessed 04 April 2015).
[2] Torresol Energy–Gemasolar Thermosolar Plant, 2015. Available from: <http://www.torresolenergy.com/TORRESOL/gemasolar.html?swlang=en> (accessed 04 April 2015).
[3] Therminol® VP-1 | Therminol, 2015. Available from: <http://www.therminol.com/products/Therminol-VP1> (accessed 23 March 2015).
[4] I. Llorente García, J.L. Álvarez, D. Blanco, Performance model for parabolic trough solar thermal power plants with thermal storage: Comparison to operating plant data, Sol. Energy 85 (2011) 2443–2460.
[5] Meteonorm, Irradiation Data for Every Place on Earth, 2015 (n.d.). Available from: <http://meteonorm.com/> (accessed 04 July 2015).
[6] C. Temstet, G. Canton, J. Laborie, A. Durante, A large high-performance MED plant in Sicily, Desalination 105 (1996) 109–114.
[7] S.A. Klein, Engineering Equation Solver Software (EES), 2013. Available from: <www.fchart.com>.
[8] A.S. Hassan, M.A. Darwish, Performance of thermal vapor compression, Desalination 335 (2014) 41–46.
[9] M.J. Montes, A. Abánades, J.M. Martínez-Val, M. Valdés, Solar multiple optimization for a solar-only thermal power plant, using oil as heat transfer fluid in the parabolic trough collectors, Sol. Energy 83 (2009) 2165–2176.
[10] R.L. Bartlett, Steam Turbine Performance and Economics, McGraw-Hill, New York, NY, 1958.
[11] A. Stodola, L.C. Loewenstein, Steam and Gas Turbines, with a Supplement on The Prospects of the Thermal Prime Mover, P. Smith, New York, NY, 1945.
[12] A.M. Patnode, Simulation and Performance Evaluation of Parabolic Trough Solar Power Plants, 2007. Available from: <http://digital.library.wisc.edu/1793/7590>.
[13] F. Lippke, Simulation of the part-load behavior of a 30 MW$_e$ SEGS plant, Tech. Rep. (1995). Available from: <http://www.osti.gov/scitech/biblio/95571>.

Appendix 1

Power block performance in on-design and off-design for only-electricity mode operation

Concept	Load = 100%	80%	50%	30%
Thermal efficiency (%)	37.89	36.6	32.94	29.09
Electrical power production (MW_e)	50	38.61	21.53	11.23
Steam mass flow rate (kg/s)	60.17	46	26.91	15.36
Steam generator thermal power (MW_{th})	115.32	93.99	60.23	36.73
Reheater thermal power (MW_{th})	21.25	15.27	8.05	4.24
Solar field thermal power (MW_{th})	140	112	70	42
Condenser thermal power (MW_{th})	83.72	68.36	45.32	28.80
Condenser pump electrical power (MW_{th})	0.052	0.033	0.016	0.008
Feeding pump electrical power (MW_{th})	0.742	0.454	0.207	0.103